Driven interfaces in random media at finite temperature : is there an anomalous zero-velocity phase at small external force ?

Cécile Monthus and Thomas Garel
Institut de Physique Théorique, CNRS and CEA Saclay, 91191 Gif-sur-Yvette cedex, France

The motion of driven interfaces in random media at finite temperature T and small external force F is usually described by a linear displacement $h_G(t) \sim V(F,T)t$ at large times, where the velocity vanishes according to the creep formula as $V(F,T) \sim e^{-K(T)/F^\mu}$ for $F \to 0$. In this paper, we question this picture on the specific example of the directed polymer in a two dimensional random medium. We have recently shown (C. Monthus and T. Garel, arXiv:0802.2502) that its dynamics for $F = 0$ can be analyzed in terms of a strong disorder renormalization procedure, where the distribution of renormalized barriers flows towards some "infinite disorder fixed point". In the present paper, we obtain that for small F, this "infinite disorder fixed point" becomes a "strong disorder fixed point" with an exponential distribution of renormalized barriers. The corresponding distribution of trapping times then only decays as a power-law $P(\tau) \sim 1/\tau^{1+\alpha}$, where the exponent $\alpha(F,T)$ vanishes as $\alpha(F,T) \propto F^\mu$ as $F \to 0$. Our conclusion is that in the small force region $\alpha(F,T) < 1$, the divergence of the averaged trapping time $\overline{\tau} = +\infty$ induces strong non-self-averaging effects that invalidate the usual creep formula obtained by replacing all trapping times by the typical value. We find instead that the motion is only sub-linearly in time $h_G(t) \sim t^{\alpha(F,T)}$, i.e. the asymptotic velocity vanishes $V = 0$. This analysis is confirmed by numerical simulations of a directed polymer with a metric constraint driven in a traps landscape. We moreover obtain that the roughness exponent, which is governed by the equilibrium value $\zeta_{eq} = 2/3$ up to some large scale, becomes equal to $\zeta = 1$ at the largest scales.

I. INTRODUCTION

A. Dynamical phase diagrams in the presence of quenched disorder

Transport phenomena in random media have remained a very active field of research since the discovery of the Anderson localization fifty years ago [1]. For classical systems also, the presence of quenched disorder can induce completely new transport behaviors with respect to pure systems in some regions of parameters. It turns out that even the dynamics of a single particle in one-dimensional random media (see the review [2] and references therein) can already present a very rich phase diagram as a function of the temperature T and the external applied force F. As an example, we shown on Fig. 1 the exactly known phase diagram for the biased Sinai model [3, 4, 5, 6] : one needs to introduce a dimensionless parameter $\alpha(F,T) = TF$ (where we have chosen to fix the disorder strength at some simple value to simplify the notations and emphasize the dependence upon T and F we are interested in). For $F = 0$, the motion is logarithmically slow $x(t) \sim \pm(\ln t)^2$. For $0 < \alpha(F,T) < 1$, the diffusion is anomalous with a sub-linear displacement $x \sim t^{\alpha(F,T)}$; for $1 < \alpha < 2$, the velocity becomes finite $x \sim Vt$, but the dispersion remains anomalous of order $t^{1/\alpha(F,T)}$. Finally for $\alpha > 2$, both the velocity and the diffusion coefficient are finite. So already in simple one-dimensional systems, various dynamical properties can undergo phase transitions at various thresholds.

The case of more complex systems like interfaces or manifolds in random media has attracted a lot of attention in relation with many important applications, and various approaches have been developed to elucidate the structure of the dynamical phase diagram (see the reviews [7, 8] and references therein). The simplest model within this class of systems is the directed polymer in a two-dimensional random medium (see [9] for a review), first introduced to model an interface in the low-temperature phase of two-dimensional disordered ferromagnets [10]. The statics of this model is rather well understood with exactly known critical exponents : at any temperature T, the directed polymer is in a disordered-dominated phase characterized by the roughness exponent $\zeta_{eq} = 2/3$ and the droplet exponent $\theta = 2\zeta_{eq} - 1 = 1/3$ [9]. In comparison, the dynamics is much harder to study, and no exact result exists. Even numerically, the computational complexity changes completely between the statics that can be studied via exact transfer matrix methods that are polynomial in the size of the polymer [9], and the dynamics where the determination of barriers is an NP-complete problem [11]. As a consequence, a complete characterization of the dynamical properties as a function of the temperature and external force (here we consider that the disorder strength is fixed) has remained a very challenging issue. An essential novelty with respect to the dynamics of the Sinai model described above, is the presence of the chain constraint of the polymer, so that even at zero temperature $T = 0$, the dynamics is already non trivial : the competition between interaction and disorder gives rise to a non-equilibrium depinning phase transition, between a pinned phase $F < F_c^{dep}$ where the interface remains blocked forever in some configuration, and a moving phase for $F > F_c^{dep}$. This type of depinning transition has motivated a lot of experimental and theoretical studies

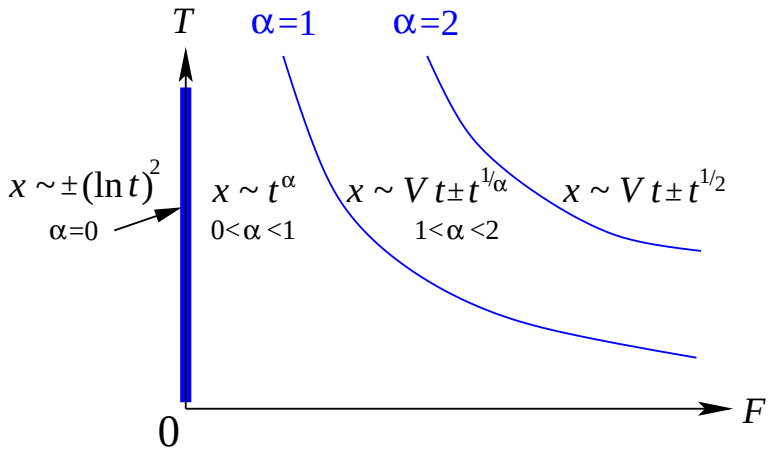

Sinai Model

FIG. 1: Exactly known dynamical phase diagram as a function of the temperature T and the external force F of the one-dimensional Sinai model [2] : the important dimensionless parameter is $\alpha(F,T) = TF$ (the disorder strength has been fixed at some simple value). From the point of view of strong disorder renormalization [29, 32, 33], the logarithmic behavior $x \sim \pm(\ln t)^2$ for $F = 0$ corresponds to an "infinite disorder fixed point", whereas the anomalous diffusion phase $x \sim t^\alpha$ for $0 < \alpha < 1$ corresponds to a "strong disorder fixed point". A finite-velocity $V > 0$ appears only for $\alpha > 1$, i.e. when the force is above some temperature-dependent value.

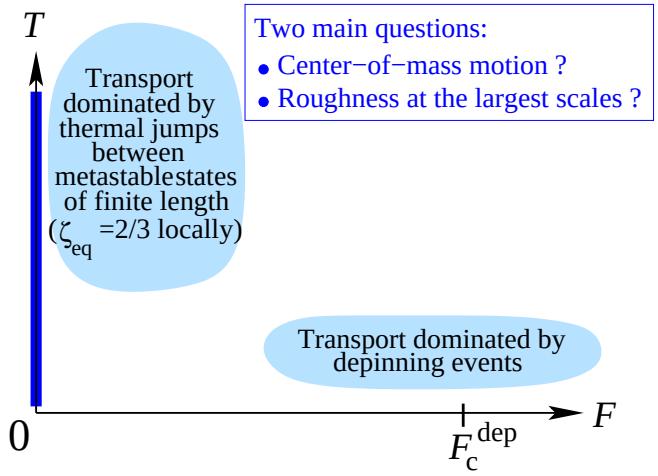

Directed Polymer Model

FIG. 2: The dynamical phase diagram for the directed polymer in a two-dimensional random medium as a function of the temperature T and the external force F is not exactly known. However one expects physically two very different regimes : (i) near the zero-temperature depinning critical point F_c^{dep}, the transport at small temperature is dominated by depinning events. (ii) in the regime where T is finite and F is small, the roughness exponent $\zeta_{eq} = 2/3$ of the equilibrium case $F = 0$ is expected to describe the polymer roughness up to some large scale (that diverges as $F \to 0$). The transport is then dominated by thermal jumps of finite segments of the polymer between quasi-equilibrated metastable states. In this paper, we focus only on the regime (ii) and discuss the center-of-mass motion and the roughness at the largest scales.

(see the reviews [7, 8]), and an exact mean-field solution has been obtained in [12]. The critical region with a small temperature around the depinning transition of an elastic line has been studied in [13].

In the present paper, we focus on the opposite region of the dynamical phase diagram (see Fig. 2) where the temperature is finite and the external force is small. In this regime, one expects that the dynamics is dominated by thermal activations between locally quasi-equilibrated metastable states. In particular, the polymer is expected to keep during the motion its equilibrium roughness exponent $\zeta_{eq} = 2/3$ up to some large scale (that diverges as $F \to 0$). This equilibrium roughness has been measured in dynamic simulations in [14], and in [15] when the temperature remains larger that some disorder-dependent threshold. However in other regimes, larger roughness exponents have been measured at larger scales [15, 16]. This issue of the roughness at the largest scales will be rediscussed later in the paper. But we first need to better understand the statistical properties of the barriers between the locally quasi-equilibrated metastable states.

B. Usual creep scenario for finite temperature and small external force

In the regime of finite temperature and small external force, the standard picture in the field (see the review [8] and references therein) seems to be that the dynamics then corresponds to a 'creep' motion, where the center-of-mass moves linearly in time as soon as the temperature is positive

$$h_G(t) \underset{t \to \infty}{\simeq} V(F,T)\ t \tag{1}$$

with a very non-linear force-velocity relation of the form

$$V(F,T) \underset{F \to 0}{\simeq} e^{-\frac{K(T)}{F^{\mu}}} \tag{2}$$

where the exponent μ involves the dimension d of the interface (the directed polymer we are interested in corresponds to $d = 1$), the equilibrium roughness exponent ζ_{eq}, and the barrier exponent ψ of the dynamics without external force

$$\mu = \frac{\psi}{(\zeta_{eq} + d - \psi)} \tag{3}$$

Note that this relation is usually written in the form $\mu_{usual} = (d - 2 + 2\zeta_{eq})/(2 - \zeta_{eq})$ after using the additional assumption concerning the identity between the barrier exponent ψ and the droplet exponent $\theta = 2\zeta_{eq} + d - 2$. However, in our opinion, there is no convincing evidence of the equality $\psi = \theta$ neither theoretically (see [17] for a recent summary on the debate) nor numerically (the best numerical results presently available [18] points towards an exponent of order $\psi \sim 0.49$ rather different from the exactly known droplet exponent $\theta = 1/3$), we will consider in the following that the barrier ψ is an independent exponent satisfying the bound

$$\psi \geq \theta \tag{4}$$

C. Summary of the present paper : alternative scenario with a zero-velocity phase at small external force

The usual qualitative argument given in favor of a finite velocity in Eq. 1 as soon as $T > 0$ is that 'any barrier can be passed by thermal activation'. This is of course true, but this is not sufficient to conclude that the asymptotic velocity is finite, since the motion can also exhibit anomalous behavior as shown by the Sinai model at small external force (see the beginning of the introduction). To determine the asymptotic motion of the center-of mass at large times, one needs to study the time needed to travel over a given large distance. The more quantitative argument in favor of the finite velocity of Eq. 1 is a scaling argument where the barrier landscape existing in the absence of bias is 'tilted' to take into account the bias contribution : this scaling argument yields that the relevant barriers for the large-time dynamics corresponds to a barrier scale $B^*(F,T)$ and to a length scale $l^*(F,T)$ that are finite as soon as $F > 0$ (and that diverge as $F \to 0$). We fully agree with this scaling argument that will be rediscussed below in section III C. However again, this is not sufficient to conclude that the velocity is finite, since exactly the same argument can be made for the Sinai model where an anomalous diffusion phase exists (see section III C for more details). The crucial property to determine whether the velocity is finite or not is the probability distribution of barriers B around this typical value $B^*(F,T)$. In the present paper, we explain that within the strong disorder renormalization in configuration space that we have introduced recently [19] (see [20] for a more detailed presentation), one obtains an exponential tail for the distribution of renormalized barriers

$$P(B) \underset{B \to +\infty}{\propto} e^{-\frac{B}{B^*(F,T)}} \tag{5}$$

As is well known in the field of disordered systems since Derrida's Random Energy Model [21], other disordered models sharing the same low-energy states statistics [22, 23] and related Bouchaud's trap Models [24] (see also [25] for one of the first mention of exponentially distributed barriers in connection with extremal statistics), this 'innocent' exponential distribution for the barriers corresponds via the change of variable $\tau = e^B$ to a very broad power-law decay for the distribution of the trapping times τ

$$P(\tau) \underset{\tau \to +\infty}{\propto} \frac{\alpha(F,T)}{\tau^{1+\alpha(F,T)}} \tag{6}$$

The exponent depends continuously on the external force and on the temperature (we consider here that the disorder remains fixed)

$$\alpha(F,T) = \frac{1}{B^*(F,T)} \tag{7}$$

Since the characteristic barrier scale $B^*(F,T)$ grows with F and diverges as $F \to 0$ as

$$B^*(F,T) \underset{F \to 0}{\propto} \frac{1}{F^\mu} \tag{8}$$

the exponent $\alpha(F,T)$ vanishes as $F \to 0$ as

$$\alpha(F,T) \underset{F \to 0}{\propto} F^\mu \tag{9}$$

As a consequence, the region of small external force where $\alpha(F,T) < 1$ corresponds to a very broad distribution of trapping times with a diverging averaged value $\overline{\tau} = +\infty$. This invalidates the usual creep formula that is obtained by replacing all trapping times by the typical value $\tau_{typ} \sim e^{B_{typ}} \sim e^{B^*(F,T)}$ to obtain $V \sim 1/\tau_{typ}$ (see Eq. 2). We obtain instead that for $\alpha(F,T) < 1$, the center-of-mass displacement then grows only sub-linearly in time

$$h_G(t) \underset{t \to \infty}{\simeq} t^{\alpha(F,T)} \tag{10}$$

i.e. the asymptotic velocity vanishes $V = 0$.

Although the vast majority of papers on the subject never mentions the possibility of a zero-velocity phase, we are aware of three papers where the question of the probability distribution of barriers around the typical value has been raised :

(i) twenty years ago, Ioffe and Vinokur [26] have proposed the anomalous sub-linear motion of Eq. 6. But for reasons that are very unclear to us, this possibility seems to have completely disappeared in the more recent literature.

(ii) fifteen years ago, Bouchaud has pointed out in [27] that the usual creep argument might lead to incorrect results because of problem of strong fluctuations, and cites the Sinai model as an example where the transport is indeed harder than anticipated from the typical barrier alone.

(ii) ten years ago, Vinokur, Marchetti and Chen [28] have proposed an exponential distribution of barriers, based on extremal statistics argument, and the corresponding power-law distribution for trapping times. However, these authors have supplemented this power-law distribution by a sharp cut-off to recover the usual finite velocity behavior of Eq. 1. In our opinion, there is no good reason to impose this sharp cut-off, since the same procedure for the exactly soluble Sinai model would give a wrong answer.

D. Organization of the paper

To summarize this long introduction, the aim of the present paper is to justify the existence of the anomalous diffusion phase of Eq. 10 in the region of the phase diagram corresponding to finite temperature and small external force (see Fig. 2), via the use of some strong disorder renormalization procedure on the barriers. The paper is organized as follows. In section II, we briefly recall the main idea of strong disorder renormalization, and we describe the statistical properties of the "infinite disorder" fixed point that describes the thermal dynamics of the directed polymer without external force. In section III, we explain how the presence of a small external force F transforms this "infinite disorder fixed point" into a "strong disorder fixed point" with an exponential distribution of renormalized barriers, and we describe the consequences for distribution of trapping times and the large-time dynamics. In Section IV, we present detailed numerical simulations for a directed polymer driven in a traps landscape. In Section V, we compare our results concerning the roughness with previous works. Our conclusions are summarized in section VI. In Appendix A, we recall the subtleties associated to the type of the interactions (metric constraint versus elastic energy) to justify our choice to consider the metric constraint.

II. PROPERTIES OF THE 'INFINITE DISORDER FIXED POINT' FOR $F = 0$

A. Strong disorder renormalization in configuration space

Strong disorder renormalization (see [29] for a review) is a very specific type of renormalization (RG) that has appeared in the field of quantum spin chains : this approach introduced by Ma and Dasgupta [30] has been developed by D.S. Fisher [31], who has introduced the crucial notion of "infinite disorder" fixed points where the method becomes asymptotically exact, and who has shown how to obtain explicit exact results for critical exponents and scaling functions for zero-temperature quantum critical points. This method has thus generated a lot of activity for various disordered quantum models [29]. It has been then successfully applied to various classical disordered dynamical models, such as random walks in random media [32, 33], reaction-diffusion in a random medium [34], coarsening dynamics of classical spin chains [35], trap models [36], random vibrational networks [37] absorbing state phase transitions [38], zero range processes [39] and exclusion processes [40]. In all these cases, the strong disorder RG rules have been formulated *in real space*, with specific rules depending on the problem. For more complex systems where the formulation of strong disorder RG rules has not been possible in real space, we have recently proposed in [19] a strong disorder RG procedure *in configuration space* that can be defined for any master equation as we now recall.

The starting point of strong disorder renormalization in configuration space is the Master Equation describing the evolution of the probability $P_t(\mathcal{C})$ to be in a configuration $\mathcal{C}$ at time t

$$\frac{dP_t(\mathcal{C})}{dt} = \sum_{\mathcal{C}'} P_t(\mathcal{C}') W(\mathcal{C}' \to \mathcal{C}) - P_t(\mathcal{C}) W_{out}(\mathcal{C}) \tag{11}$$

The notation $W(\mathcal{C}' \to \mathcal{C})$ represents the transition rate from configuration $\mathcal{C}'$ to $\mathcal{C}$, and the notation

$$W_{out}(\mathcal{C}) \equiv \sum_{\mathcal{C}'} W(\mathcal{C} \to \mathcal{C}') \tag{12}$$

represents the total exit rate out of configuration $\mathcal{C}$.

For dynamical models, the aim of any renormalization procedure is to integrate over 'fast ' processes to obtain effective properties of 'slow' processes. The general idea of 'strong renormalization' for dynamical models consists in eliminating iteratively the 'fastest' process. The RG procedure introduced in [19] consists in the iterative elimination of the state with the highest exit rate. We refer to [19, 20] for a detailed description and derivation of the renormalization rules on the transition rates. Their most important property is their multiplicative structure that suggests that for a very broad class of disordered systems, the distribution of renormalized exit barriers

$$B_{out} \equiv -\ln W_{out} \tag{13}$$

will become broader and broader upon iteration, so that the strong disorder renormalization procedure should become asymptotically exact at large time scales. Note that a very important advantage of this formulation in terms of the transition rates of the master equation is that the renormalized barriers take into account the true 'barriers' of the dynamics, whatever their origin which can be either energetic or entropic.

After this general presentation (see [19, 20] for more details), we now turn to the specific problem of a directed polymer in a two-dimensional random medium we are interested in. For the dynamics *without external force*, we have followed numerically the RG flow of the renormalized transition rates and we have found some "infinite disorder" fixed point [19, 20] as we now explain.

B. Distribution of renormalized exit barriers at large scale

The RG scale Γ is defined as the scale of the last eliminated exit barrier. At time t, the appropriate RG scale is thus

$$\Gamma(t) = \ln t \tag{14}$$

so that all metastable states of exit barrier $B_{out} > \Gamma$, i.e. of exit time $\tau = e^{B_{out}} > t$ have been kept, whereas all metastable states of exit time $\tau = e^{B_{out}} < t$ have been eliminated. At large scale, one expects that the probability distribution of the remaining exit barriers $B_{out} \geq \Gamma$ will converge towards some scaling form

$$P_\Gamma(B_{out}) \underset{\Gamma \to \infty}{\simeq} \frac{1}{\sigma(\Gamma)} \hat{P}\left(\frac{B_{out} - \Gamma}{\sigma(\Gamma)}\right) \tag{15}$$

where $\hat{P}$ is the fixed point probability distribution, and where $\sigma(\Gamma)$ is the appropriate scaling factor that represents the width of the renormalized distribution.

For the directed polymer in a two-dimensional random medium, we have obtained numerically in [19, 20] that the width $\sigma(\Gamma)$ grows asymptotically linearly with the RG scale Γ

$$\sigma(\Gamma) \underset{\Gamma \to \infty}{\simeq} \Gamma \tag{16}$$

and that the rescaled distribution of Eq. 15 is extremely close to the exponential form

$$\tilde{P}(x) \simeq e^{-x} \tag{17}$$

Note that these two properties seem extremely robust within strong disorder RG since they hold for exactly in soluble models in $d = 1$ [29] and have been also found numerically in quantum models in dimension $d > 1$ [41].

C. Scaling between barriers and length scales

To describe the thermal relaxation of disordered systems towards equilibrium when starting at time $t = 0$ from a non-equilibrium initial state, it is useful to introduce the notion of some coherence length $l_T(t)$ that grows slowly in time (see the reviews [42, 43] and references therein). This coherence length separates the smaller lengths $l < l_T(t)$ which are quasi-equilibrated at time t from the larger lengths $l > l_T(t)$ which are completely out of equilibrium. Then full equilibrium is reached only when the coherence length reaches the macroscopic linear size $l_T(t_{eq}) = L$ of the system. Within the droplet scaling theory proposed both for spin-glasses [44, 45] and for directed polymers in random media [46], the barriers grow as a power law of the length l

$$B(l) \sim l^{\psi} \tag{18}$$

with some barrier exponent $\psi > 0$. The typical time $t_{typ}(L)$ associated to scale l grows as an exponential $\ln t_{typ}(l) \sim B(l) \sim l^{\psi}$. Equivalently, the coherence length-scale $l_T(t)$ associated to time t grows only logarithmically in time

$$l_T(t) \sim (\ln t)^{\frac{1}{\psi}} \tag{19}$$

In the numerical study of the relaxation towards equilibrium of an elastic chain in a two dimensional random medium, starting from a straight line at $t = 0$, this coherence length can be extracted from the behavior of the structure factor as a function of time [18], and the corresponding measure of the barrier exponent yields $\psi \sim 0.49$ [18] (see the comments on this exponent ψ before Eq. 4).

Within the strong disorder renormalization procedure, one may either extract a coherence length l_Γ as a function of the RG scale [20], or consider the statistics of the barriers associated to a given length [19, 20], and one obtains the scaling

$$B(l) \underset{l \gg 1}{\simeq} \Delta(T) l^{\psi} u \tag{20}$$

where u is a random variable of order one. The barrier exponent ψ obtained in [20] is of order $\psi \sim 0.47$, i.e. close to the estimation $\psi \sim 0.49$ measured in [18] via Langevin dynamics. A systematic study of the dependence of the prefactor $\Delta(T)$ upon temperature is not yet available. This prefactor would be of the form C/T if the barriers were purely energetic, but since the strong disorder renormalization is defined on the transition rates, the prefactor $\Delta(T)$ may also contain entropic contributions and then have a more complicated temperature dependence.

D. Final picture for the dynamics at $F = 0$

The final picture for the dynamics of the directed polymer of length L at finite temperature T and no external force $F = 0$ is thus the following :

(a) during the regime $l_T(t) < L$ where the coherence length $l_T(t)$ is smaller than the length L of the polymer, the polymer is quasi-equilibrated with its equilibrium roughness exponent $\zeta_{eq} = 2/3$ only on smaller length scale than the coherence length $l < l_T(t)$, whereas larger length scale $l > l_T(t)$ are still completely out-of-equilibrium. The "infinite disorder fixed point" describes the hierarchical structure of growing barriers that have to be passed to equilibrate on larger and larger length scales, and this is why the coherence length grows only logarithmically in time

$$l_T(t) \sim \left(\frac{\ln t}{\Delta(T)} \right)^{\frac{1}{\psi}} \tag{21}$$

(b) when the coherence length $l_T(t)$ reaches the length L of the polymer, the full polymer is characterized by the equilibrium roughness exponent $\zeta_{eq} = 2/3$. The coherence length $l_T(t)$ cannot grow anymore, so that the renormalization procedure has to be stopped at the RG scale of order

$$\Gamma_L \sim \Delta(T) L^{\psi} \tag{22}$$

One then expects that the polymer of roughness exponent $\zeta_{eq} = 2/3$ will become able to move slowly in the transversal direction between metastable states that are separated by distances of order $L^{\zeta_{eq}}$ and by barriers distributed with the fixed point distribution (Eq. 15, 16 and 17) for the scale Γ_L, that presents the exponential decay

$$P_{\Gamma_L}(B_{out}) \underset{B_{out} \to \infty}{\simeq} \frac{1}{\Gamma_L} e^{-\frac{B_{out}}{\Gamma_L}} \tag{23}$$

On the renormalized scale Γ_L, one expects that the transverse motion of the center-of-mass corresponds to an effective one-dimensional Sinai model, where the unit distance scale is of order $L^{\zeta_{eq}}$ and the unit barrier scale is $\Gamma_L \sim \Delta(T) L^{\psi}$. As a consequence for $\ln t \gg \Delta(T) L^{\psi}$, one expects the logarithmically slow behavior

$$h_G(t) \simeq \pm L^{\zeta_{eq}} \left(\frac{\ln t}{\Delta(T) L^{\psi}} \right)^2 \tag{24}$$

III. PROPERTIES OF THE 'STRONG DISORDER FIXED POINT' FOR SMALL FORCE F

A. Analysis of the RG flow for small F

The "infinite disorder fixed point" described above for $F = 0$ characterizes some 'criticality' in the time direction in the following sense : there is no characteristic scale for the barriers except the RG scale Γ itself. This scale invariance will be broken by the introduction of some external force F that will introduce some characteristic length-scale and thus some corresponding scale $B^*(F,T)$ for the barriers. However, if the external force is very small, the scale $B^*(F,T)$ (that diverges as $F \to 0$) will be very large. We thus expect that the RG flow can be analyzed in terms of two regimes :

(i) during the first regime $1 \ll \Gamma \leq B^*(F,T)$, the distribution of the renormalized exit barriers will follow the same RG flow as in the absence of force, i.e. it will converge towards the scaling of Eq. 15, with the same exponential rescaled distribution of Eq. 17

$$P_{\Gamma,F,T}(B_{out}) \simeq \frac{1}{\sigma(\Gamma,F,T)} e^{-\frac{(B_{out}-\Gamma)}{\sigma(\Gamma,F,T)}} \tag{25}$$

with a width $\sigma(\Gamma,F,T)$ which grows linearly in Γ as in Eq. 16

$$\sigma(\Gamma,F,T) \underset{1 \ll \Gamma \ll B^*(F,T)}{\simeq} \Gamma \tag{26}$$

(ii) when the large scale $\Gamma \sim B^*(F,T)$ is reached, the width saturates at the finite large value $B^*(F,T)$

$$\sigma(\Gamma,F,T) \underset{\Gamma \geq B^*(F,T)}{\simeq} B^*(F,T) \tag{27}$$

instead of the flow towards infinity that characterizes the critical case $F = 0$. Since this width remains finite asymptotically as $\Gamma \to \infty$, one speaks of a 'finite-disorder fixed point'. However, since this width $B^*(F,T)$ diverges at small force , the region of small F is a 'strong disorder fixed point', where the asymptotic accuracy of the renormalization approach is of order $1/B^*(F,T)$. This notion is thus very useful to study the vicinity of 'infinite disorder fixed point' in the space of parameters and we refer to the review [29] for more detailed discussions. In one-dimension, where the strong disorder RG procedure can be followed exactly, the crossover of the width between the regimes (i) and (ii) described above, is of the form (translated in our present notation) : $\sigma(\Gamma,F,T) = B^*(F,T) \left[1 - e^{-\frac{\Gamma}{B^*(F,T)}} \right]$ [29, 31].

For our present analysis, the important point is that the saturation scale $B^*(F,T)$ is large enough, so that the RG flow during the first regime $1 \ll \Gamma \ll B^*(F,T)$, that behaves as the critical flow, contains sufficiently RG steps to have converged towards the scaling form of Eq. 25. So, when saturation occurs at scale $B^*(F,T)$, the probability distribution of renormalized exit barrier follows the exponential form

$$P_{\Gamma}(B) \simeq \frac{1}{B^*(F,T)} \; e^{-\frac{(B-\Gamma)}{B^*(F,T)}} \tag{28}$$

B. Physical meaning of the saturation

The physical meaning of the two regimes described above is as follows. During the first regime (i), the external force F is so small that the flow is very similar to the flow for $F = 0$. In particular, the barriers grows upon iteration on scales $1 \ll \Gamma \ll B^*(F,T)$ and the motion is not yet directed along the bias. When the saturation occurs at the large scale $B^*(F,T)$, this means on the contrary that the motion becomes effectively directed in the direction of the external force F for scales $\Gamma > B^*(F,T)$. The barriers against the bias are not renormalized anymore, and one can stop the renormalization procedure. The appropriate model on this scale is then a directed model along the bias, with barriers distributed as in Eq. 28. As recalled in the introduction (see the discussion between Eqs. 5 and 6), the corresponding distribution of the trapping time $\tau = e^B$ is then a broad power law

$$P(\tau) \simeq \frac{1}{\tau^{1+\alpha(F,T)}} \tag{29}$$

with exponent

$$\alpha(F,T) = \frac{1}{B^*(F,T)} \tag{30}$$

C. Determination of the saturation scale $B^*(F,T)$

Within our present RG framework, the saturation scale $B^*(F,T)$ should be determined as the limiting value of the width (Eq. 27) of the renormalized distribution of barriers. To determine the dependence on the external force at small F, we may rephrase the scaling argument which is usually used in the field [8] as follows. On the length scale l, the barriers *in the absence of external force* follow the scaling of Eq. 20 with the barrier exponent ψ. If the external force F is small, one may take into account its effects by a 'tilt' of the landscape that lowers the barriers against the force in the following way

$$B(l) \underset{l \gg 1}{\simeq} \Delta(T) l^{\psi} u - \frac{F}{T} l^{1+\zeta_{eq}} \tag{31}$$

where ζ_{eq} represents the equilibrium roughness exponent, so that the correction in Eq. 31 corresponds to a transversal move of order $l^{\zeta_{eq}}$ for the segment of length l of the polymer. Since $(1+\zeta_{eq}) > \psi$, the force term always dominates at sufficiently large length scale. The length scale $l^*(F,T)$ that will give rise to the biggest barriers can be obtained by differentiating Eq. 31 with respect to l. Dropping constants of order $O(1)$ one obtains the length scale

$$l^*(F,T) \underset{F \to 0}{\simeq} \left(\frac{T\Delta(T)}{F} \right)^{\frac{1}{(\zeta_{eq}+1-\psi)}} \tag{32}$$

and the corresponding barrier scale

$$B^*(F,T) \underset{F \to 0}{\simeq} \Delta(T) \left(\frac{T\Delta(T)}{F} \right)^{\mu} \tag{33}$$

where μ is the exponent that usually appear in the creep formula (see Eq. 3 and associated comments)

$$\mu \equiv \frac{\psi}{(\zeta_{eq}+1-\psi)} \tag{34}$$

So the power-law exponent of Eq. 30 vanishes for $F \to 0$ as

$$\alpha(F,T) = \frac{1}{B^*(F,T)} \underset{F \to 0}{\simeq} \frac{1}{\Delta(T)} \left(\frac{F}{T\Delta(T)} \right)^{\mu} \tag{35}$$

In the case of the Sinai model, one may actually use exactly the same arguments with the following changes : the length l is now along the direction of the motion, the barrier exponent $\psi = 1/2$ simply describes the Brownian fluctuation of the random energy landscape, the prefactor $\Delta(T)$ has the simple T-dependence $\Delta(T) = C/T$ because the barriers are purely energetic, and there is no roughness exponent $\zeta_{eq} = 0$ since the model concerns a single particle. For this special case, one obtains $\mu = 1$ and the following expression for the power-law exponent

$$\alpha_{Sinai}(F,T) \propto TF \tag{36}$$

in agreement with the exact results mentioned at the beginning of the introduction.

D. Final picture for the dynamics at small external force F

In the case of the Sinai model, the saturation scales $l^*(F,T)$ for the length and $B^*(F,T)$ for the barrier are the only finite scales present in the problem. The strong disorder renormalization procedure should then be stopped at the scale $B^*(F,T)$, and one ends up with an effective directed trap model. We refer to [33] for a more detailed presentation of the quantitative relations that can be derived at large scales between the Sinai model in an external force and the one-dimensional directed trap model.

For the present model concerning the directed polymer, the polymer length L introduces another length scale in the problem. Of course, one is interested into large polymer length $L \gg 1$, but since the length $l^*(F,T)$ diverges as $F \to 0$ (Eq. 32), one needs to distinguish various regimes in terms of the polymer length L

1. *Regime* $1 \ll L \ll l^*(F,T)$

In the regime $1 \ll L \ll l^*(F,T)$, the relevant barriers for the motion of the polymer as a whole corresponds to the RG scale Γ_L of Eq. 22, which is well below the saturation scale $B^*(F,T)$ introduced by the force F. This means that the force F is then too small to impose a directed motion between two neighboring quasi-equilibrated metastable configurations. The motion will become effectively directed only on larger transversal lengthscales separating many metastable configurations.

2. *Regime* $L \sim l^*(F,T)$

For a polymer of length of order $L \sim l^*(F,T)$, the motion of the polymer corresponds to an effectively directed trap model. Each trap of trapping time τ_i corresponding to a transverse displacements of order $x_i = (l^*(F,T))^\zeta X_i$ (where X_i is a random variable of order $O(1)$ with a finite averaged value $\overline{X_i} < \infty$). After n traps, the total displacement of the center of mass will be of order

$$h_G(n) = x_1 + x_2 + ... + x_n \underset{n\to\infty}{\simeq} n\,[l^*(F,T)]^\zeta \tag{37}$$

whereas the total time needed to escape from these n traps will be of order

$$t(n) = \tau_1 + \tau_2 + ... + \tau_n \tag{38}$$

As is well known in the field of Lévy statistics [2], the sum of n variables distributed with the broad power-law of Eq. 29 grows linearly in n only when the average value $\overline{\tau}$ remains finite, i.e. for $\alpha > 1$

$$t(n) \underset{n\to\infty}{\simeq} n\overline{\tau} \ \text{ if } \ \alpha(F,T) > 1 \tag{39}$$

However for $\alpha < 1$, the average value of the trapping time diverges $\overline{\tau} = +\infty$ and the sum grows more rapidly as

$$t(n) \underset{n\to\infty}{\simeq} n^{\frac{1}{\alpha}} \ \text{ if } \ \alpha(F,T) < 1 \tag{40}$$

It is then clear that the asymptotic velocity is finite only for $\alpha(F,T) > 1$. For $\alpha(F,T) < 1$, the velocity vanishes $V = 0$ and the center-of-mass displacement grows only sub-linearly in time

$$h_G(t) \underset{t\to\infty}{\simeq} t^{\alpha(F,T)} \ \text{ if } \ \alpha(F,T) < 1 \tag{41}$$

3. *Regime* $L \gg l^*(F,T)$

Finally in the regime $L \gg l^*(F,T)$, the strong disorder RG procedure has to be stopped at the RG scale $B^*(F,T)$ of Eq. 33 corresponding to the length scale $l^*(F,T)$ of Eq. 32. The picture that emerges is then some kind of directed 'parallel' trap model, where a number of order $L/l^*(F,T)$ segments of typical length $l^*(F,T)$ have to move in parallel in a trap landscape where the statistics of trapping times is given by the broad power-law of Eq. 29 with exponent given in Eq. 35. The main question is then to determine the form of the effective interaction between these large segments from the knowledge of the microscopic interactions between monomers. This issue is discussed in detail in Appendix A, where we first recall why the metric constraint is a safe choice for the microscopic interactions (in

contrast with a quadratic elastic energy that is known to lead to an unphysical roughness exponent in some cases), and where we then explain why the metric constraint is also an appropriate choice for the effective interactions between consecutive segments of size $l^*(F,T)$.

From the two properties :

(i) each segment of size $l^*(F,T)$ would follow the sub-linear motion of Eq. 41 if it were alone

(ii) the metric constraint between these segments can only delay (but not accelerate) each segment with respect to the motion it would have followed if it had been alone

we conclude that the center-of-mass motion will also follow the asymptotic sublinear behavior of Eq. 41

$$h_G(t) \underset{t\to\infty}{\simeq} t^{\alpha(F,T)} \quad \text{if} \quad \alpha(F,T) < 1 \tag{42}$$

This is confirmed by the numerical simulations presented in the next section, where we moreover discuss the behavior of the interface width at the largest scales (i.e. at scales much larger than $l^*(F,T)$ for the initial microscopic model).

IV. NUMERICAL STUDY OF A DIRECTED POLYMER DRIVEN IN A TRAPS LANDSCAPE

In this section, we define and study an effective directed model within a landscape made of traps, which is expected to be the appropriate coarse-grained model of the true microscopic non-directed dynamics in the regime $L \gg l^*(F,T)$ discussed above in section III D 3. We stress that a single monomer of this effective model represents a quasi-equilibrated segment of length $l^*(F,T)$ of internal roughness $\zeta_{eq} = 2/3$ of the true microscopic model (see the previous sections for more explanations).

A. Definition of the effective directed model within a traps landscape

We consider a directed polymer of length L defined by the heights $(h_1, h_2, ..., h_L)$ with cyclic boundary conditions $h_{L+1} \equiv h_1$ and with the metric constraint

$$|h_{i+1} - h_i| = \pm 1 \tag{43}$$

The initial configuration is the 'flat' zig-zag configuration

$$\begin{aligned} h_{2i} &= 1 \\ h_{2i+1} &= 0 \end{aligned} \tag{44}$$

The traps landscape is defined as follows : the random trapping times $\tau(i,h_i)$ are independent and drawn from the power-law distribution

$$q(\tau) = \theta(\tau > 1)\frac{\alpha}{\tau^{1+\alpha}} \tag{45}$$

The dynamics is defined by a Master Equation of the form of Eq. 11. To respect the chain constraints of Eq. 43, the monomer (i) of the configuration $\mathcal{C} = (h_1, h_2, ..., h_L)$ is 'movable' only if $h_{i-1} = h_i + 1 = h_{i+1}$, and the possible movement is then $h_i \to h_i + 2$. The total rate out of the configuration $\mathcal{C}$ is thus given by

$$W_{out}(\mathcal{C} = \{h_1, h_2, ..., h_L\}) = \sum_{i=1}^{L} W_i(\mathcal{C}) \tag{46}$$

$$W_i(\mathcal{C} = \{h_1, h_2, ..., h_L\}) = \frac{\delta_{h_{i-1},h_i+1}\ \delta_{h_{i+1},h_i+1}}{\tau(i,h_i)} \tag{47}$$

The two main observables in the field of interface dynamics are [49]

(i) the height $h_G(t;L)$ of the center-of-mass of an interface of length L as a function of time t

$$h_G(t;L) = \frac{1}{L}\sum_{i=1}^{L} h_i(t) \tag{48}$$

(ii) the width $w(t)$ of the interface of length L as a function of time t

$$w^2(t;L) = \frac{1}{L}\sum_{i=1}^{L} [h_i(t) - h_G(t)]^2 \tag{49}$$

B. Numerical details

In our numerical study, we have used the 'Bortz-Kalos-Lebowitz algorithm' [47] which is a faster-than-the-clock algorithm where each program iteration computes the time and the site where the next movement occurs [48]. The idea is that from the knowledge of W_{out}, the escape time t_{esc} from configuration $\mathcal{C}$ is a random variable drawn from the law

$$P_{\mathcal{C}}^{exit}(t_{esc}) = W_{out}(\mathcal{C}) e^{-W_{out}(\mathcal{C}) t_{esc}} \tag{50}$$

Then the monomer (i) which is effectively moved $h_i \to h_i + 2$ is drawn with the probability

$$\pi(i) = \frac{W_i(\mathcal{C})}{W_{out}(\mathcal{C})} \tag{51}$$

In this framework, the total displacement h_G of the center-of-mass is the natural variable, and one computes for a given dynamics in a given disordered sample the time $t(h_G)$ needed to reach a given displacement h_G of the center-of-mass. Similarly, one computes the width $w(h_G)$ of the interface for a given displacement h_G of the center-of-mass starting from the flat initial condition of Eq. 44. The numerical results presented below correspond to measures at the values $h_G = 2, 4, ...h_G^{max}$, where the maximal displacement h_G^{max} wished at the end of the simulation fixes the CPU time.

For the case $\alpha = 0.5$ where the averaged trapping time diverges $\overline{\tau} = +\infty$ (Eq 45), we have made studies with $h_G^{max} \sim L$ and with $h_G^{max} \sim L^{1.5}$ for the following sizes and the corresponding number $n_s(L)$ of disordered samples :

(i) for $h_G^{max} \sim L$, we have studied sizes in the range $10^3 \leq L \leq 24.10^3$ with a statistics between $n_s(L = 10^3) = 4.10^5$ and $n_s(L = 24.10^3) = 1600$.

(ii) for $h_G^{max} \sim L^{1.5}$, we have studied sizes in the range $10^2 \leq L \leq 4.10^3$ with a statistics between $n_s(L = 10^2) = 3.10^6$ and $n_s(L = 4.10^3) = 500$.

For the case $\alpha = 2$ where the averaged trapping time is finite $\overline{\tau} < +\infty$ (Eq 45), we have made studies with $h_G^{max} \sim L$ for sizes between $10^2 \leq L \leq 10^4$ with a statistics between $n_s(L = 10^2) = 4.10^5$ and $n_s(L = 10^4) = 1600$. (Note that all other parameters being the same, the CPU time turns out to be larger for the case $\mu = 2$ than for the case $\mu = 0.5$, because the number of 'movable monomers' in the stationary regime is larger for the case $\mu = 2$)

We give below results for single histories in a given disordered sample, as well as disorder-averaged results denoted by an overbar. In particular, we will be interested in $\overline{\ln t(h_G)}$ that represents the disorder-average of the logarithm of the time needed to reach a displacement h_G of the center-of-mass. For the width defined in Eq. 49, we moreover introduce the following notation

$$w_{av}(t, L) \equiv \left(\overline{w^2(t; L)} \right)^{1/2} \tag{52}$$

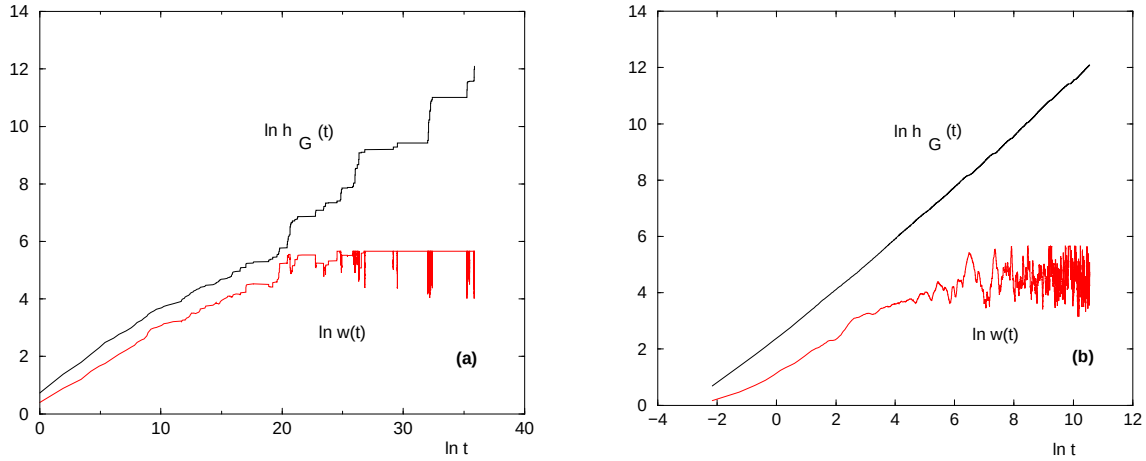

FIG. 3: (Color online) Typical dynamics of a single interface : log-log plot of the center-of-mass height $h_G(t)$ and of the interface width $w(t)$ as a function of the time t time for a polymer of length $L = 2000$ (a) for the case $\alpha = 0.5$ where the averaged trapping time diverges $\overline{\tau} = +\infty$ (Eq 45), the dynamics is very intermittent. (b) for the case $\alpha = 2$ where the averaged trapping time is finite $\overline{\tau} < +\infty$ (Eq 45), the center-of-mass motion is smooth.

C. Typical dynamics of a single interface

We first consider a single history in a given disordered sample for a polymer of length $L = 2000$. The dynamics of the center-of-mass position $h_G(t)$ (Eq. 48) and of the width $w(t)$ (Eq. 49) are shown on Fig. 3 (a) for the case $\alpha = 0.5$ where the averaged trapping time diverges $\overline{\tau} = +\infty$ (Eq 45), and on Fig. 3 (b) for the case $\alpha = 2$ where the averaged trapping time is finite $\overline{\tau} < +\infty$ (Eq 45). This comparison shows that the dynamics is very different in the two cases. For $\alpha = 0.5$, the stationary regime is characterized by a very intermittent dynamics of the center-of-mass $h_G(t)$ and of the width $w(t)$, which remain pinned for long time intervals separated by rapid avalanches. On the contrary for $\alpha = 2$, the motion of the center-of-mass is smooth, and in the stationary regime, the width $w(t)$ fluctuates rapidly around its time-averaged value.

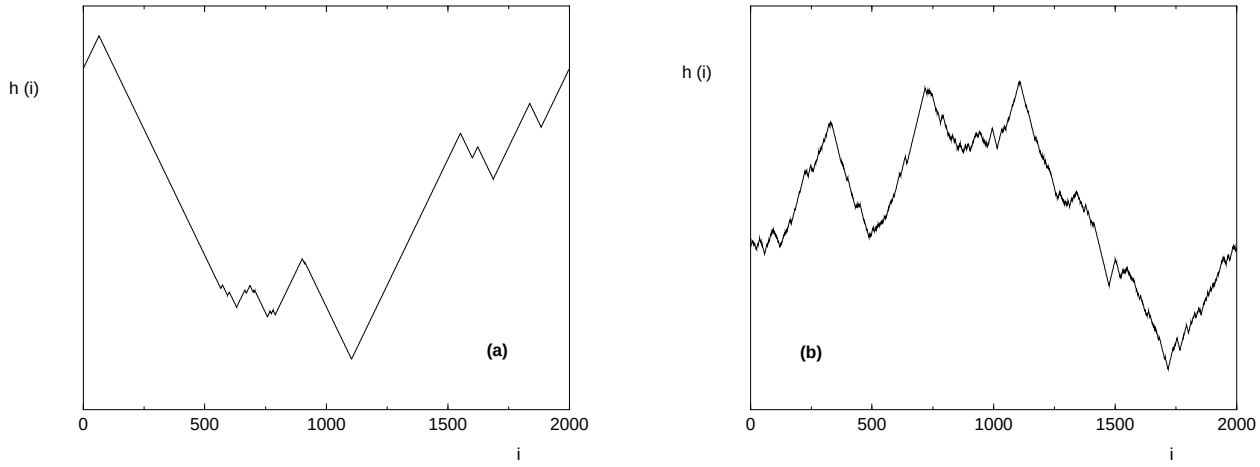

FIG. 4: (Color online) Typical configurations in the stationary regime for a polymer of length $L = 2000$ (a) for the case $\alpha = 0.5$ where the averaged trapping time diverges $\overline{\tau} = +\infty$ (Eq 45), very large regions of slope 1 are present (b) for the case $\alpha = 2$ where the averaged trapping time is finite $\overline{\tau} < +\infty$ (Eq 45) , there are more structures on shorter scales.

We show on Fig. 4 typical corresponding configurations in the stationary regime. For $\alpha = 0.5$, one clearly see on Fig. 4 (a) very large regions of slope 1, whereas for $\alpha = 2$, the configuration of Fig. 4 (b) presents more structures on shorter scales.

D. Disorder-averaged behaviors for a given size L

We have shown above on Fig 3 the dynamics of $h_G(t)$ and $w(t)$ for a single history of a polymer of size L. We show on Fig. 5 the same observables after averaging over $n_s = 2000$ disordered samples.

We note $t^*(L)$ the crossover time between the transient regime where the disorder-averaged width $w_{av}(t, L)$ (Eq. 52) grows and the stationary regime where the disorder-averaged width saturates towards a time-independent value

$$w_{av}(t, L) \underset{t \gg t^*(L)}{\simeq} w_{sat}(L) \tag{53}$$

For $\alpha = 0.5$, we find that in the stationary regime, the plot of $\ln h_G$ as a function of $\overline{\ln t(h_G)}$ (see Fig. 5 a) corresponds to a slope 0.5

$$\ln h_G \underset{t \gg t^*(L)}{\simeq} 0.5 \ln t + ... = \alpha \ln t + ... \tag{54}$$

in agreement with the sub-linear motion predicted in Eq. 42. Of course for $\alpha = 2$ we find that in the stationary regime, the plot of $\ln h_G$ as a function of $\ln t$ (see Fig. 5 b) corresponds to a slope 1 corresponding to the usual case of finite velocity $h_G(t) \sim Vt$.

For $\alpha = 0.5$, we moreover measure that, in the initial transient regime, the center-of-mass and the width both grows with the same exponent β in time

$$\begin{aligned} \ln h_G(t, L) &\underset{t \ll t^*(L)}{\simeq} \beta \ln t + ... \\ \ln w_{av}(t, L) &\underset{t \ll t^*(L)}{\simeq} \beta \ln t + ... \end{aligned} \tag{55}$$

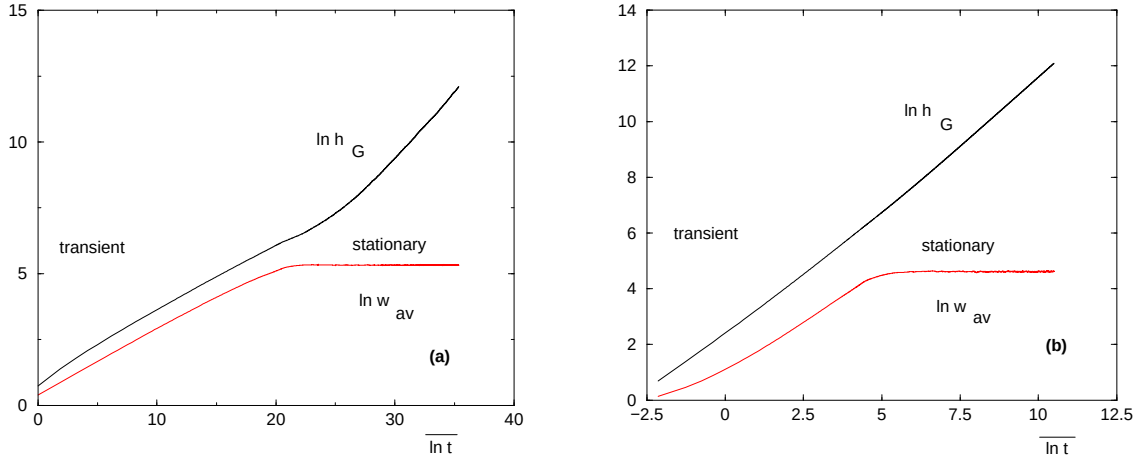

FIG. 5: (Color online) Disorder-averaged properties of the center-of-mass height h_G and of the interface width w as a function of time (log-log plot) : data averaged over $n_s = 2000$ disordered samples for a polymer of length $L = 2000$ (a) for the case $\alpha = 0.5$ where the averaged trapping time diverges $\overline{\tau} = +\infty$ (Eq 45), the center-of-mass motion is sublinear with exponent $\beta \sim 0.25$ in the transient regime (Eq. 55) and with exponent $\alpha = 0.5$ in the stationary regime (Eq. 54) (b) comparison with the case $\alpha = 2$ where the averaged trapping time is finite $\overline{\tau} < +\infty$ (Eq 45).

with a value of order

$$\beta \sim 0.24 \tag{56}$$

that will be interpreted in section IV G below.

E. Roughness exponent in the stationary regime

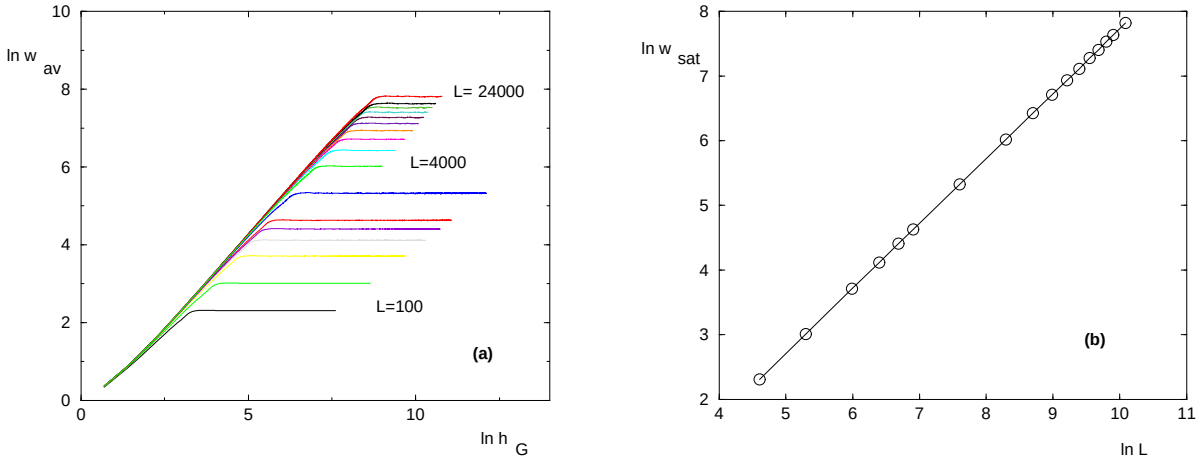

FIG. 6: (Color online) Dynamics of the width of the interface for $\alpha = 0.5$: (a) $\ln w_{av}$ as a function of $\ln h_G$ for various sizes L (b) $\ln w_{sat}(L)$ as a function of $\ln L$: the slope corresponds to the roughness exponent $\zeta = 1$.

We now consider the dynamics of the disorder-averaged width defined in Eq. 52 as a function of the center-of-mass displacement h_G.

For $\alpha = 0.5$, we show on Fig. 6 (a) the dynamics of the width w_{av} for various polymer sizes L. We show on Fig. 6 (b) the log-log plot of the saturation value $w_{sat}(L)$ defined in Eq. 53 as a function of L : we find a slope of order 1

$$\ln w_{sat}(L) \simeq \ln L + ... \tag{57}$$

Our conclusion is thus that for $\alpha < 1$, the roughness exponent is $\zeta = 1$, as already suggested by the shape of typical configurations in the stationary regime (see Fig. 4 a)

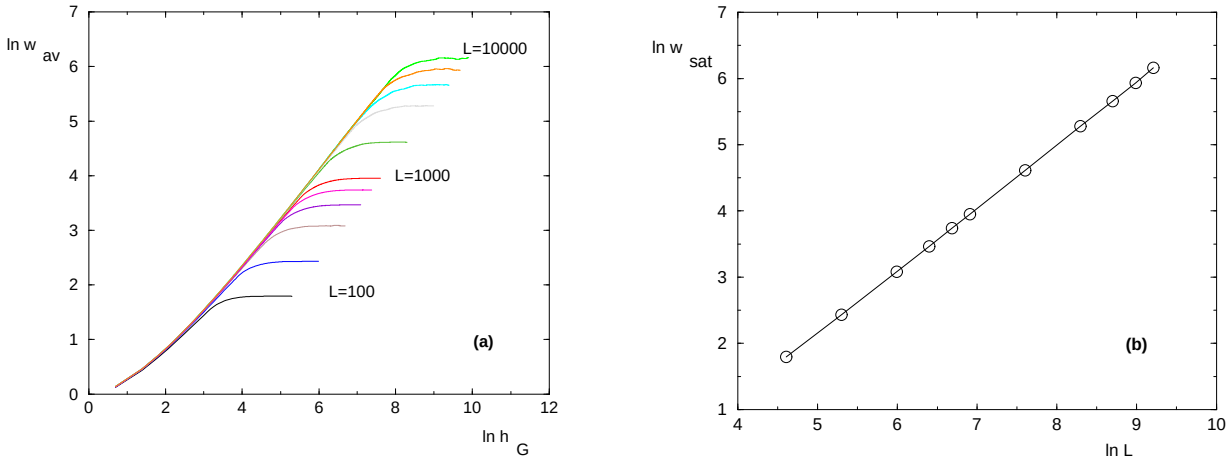

FIG. 7: (Color online) Dynamics of the width of the interface for $\alpha = 2$ (a) $\ln w_{av}$ as a function of $\ln h_G$ for various sizes L (b) $\ln w_{sat}(L)$ as a function of $\ln L$: the slope is of order 0.95.

For comparison, we show on Fig. 7 the same observables for the case $\alpha = 2$. In particular, the log-log plot of Fig. 7 (b) corresponds to a slope of order $\ln w_{sat}(L) \sim 0.95 \ln L$ for the width in the stationary regime. This high value can be understood from the typical configuration in the stationary regime shown on Fig. 4 b. This suggests that even in the finite velocity phase $\alpha > 1$ where the averaged trapping time is finite (Eq 45), it is very difficult for the different regions of the polymer to remain synchronized during the dynamics, so that the the polymer tends to be stretched on large distances with a slope close to the maximal slope 1 allowed in the presence of the metric constraint.

F. Finite-size scaling forms in t and L in the case $\alpha < 1$

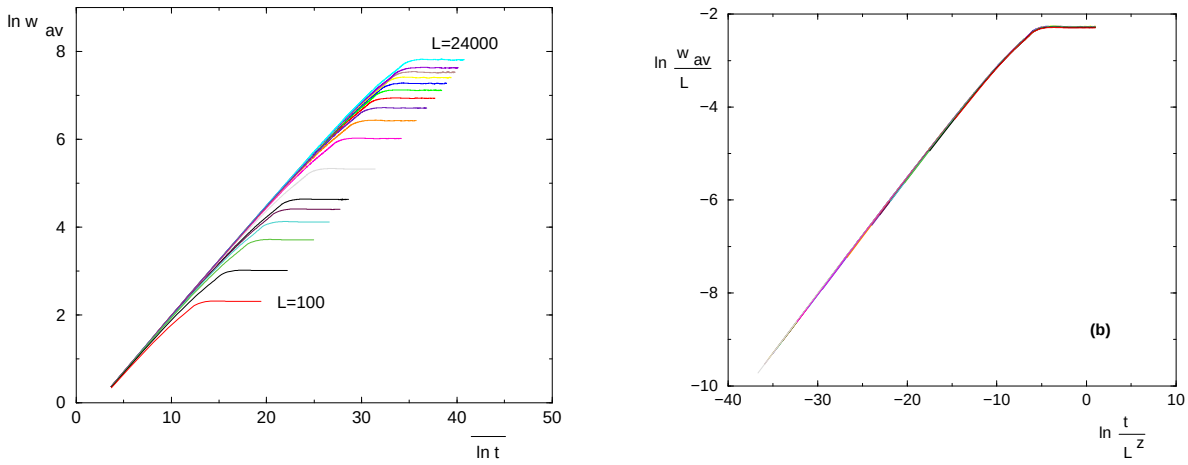

FIG. 8: (Color online) Finite-size scaling analysis in t and L the width of the interface in the case $\alpha = 0.5$: (a) $\ln w_{av}$ as a function of $\ln t$ for various sizes L (b) Data collapse of the same data using the variables $\ln(w_{sat}(L)/L)$ as a function of $\ln(t/L^z)$ (see Eq. 58) with $z = 4$.

In the field of interface dynamics, it is usual to summarize the crossover between the transient dynamics and the stationary dynamics by the following scaling form for the width [49]

$$w_{av}(t;L) \simeq L^{\zeta} \phi\left(\frac{t}{L^z}\right) \tag{58}$$

where ζ represents the roughness in the stationary regime, where z is the dynamical exponent of the crossover time $t^*(L) \sim L^z$ and where the scaling function $\phi(x)$ has the following behaviors :

(i) it converges towards a constant at infinity $\phi(x \to \infty) \sim const$ to recover the saturation value (Eq. 53) at large time ;

(ii) it behaves as a power-law at small argument : $\phi(x \to 0) \sim x^{\beta}$ where the exponent β governs the growth in time during the initial transient behavior

$$w_{av}(t;L) \underset{t \ll L^z}{\simeq} L^{\zeta - \beta z} t^{\beta} \sim t^{\beta} \tag{59}$$

where the scaling relation $\zeta = \beta z$ between exponents is expected to obtain a L-independent behavior in the transcient regime [49].

We show on Fig. 8 that a good data collapse can be achieved with the values $\zeta = 1$ and

$$z(\alpha = 0.5) \simeq 4 \tag{60}$$

The corresponding exponent of the scaling function $\phi(x)$ at small argument is measured to be of order

$$\beta(\alpha = 0.5) \simeq 0.24 \tag{61}$$

in agreement with the previous estimate of Eq. 56.

Equivalently, as a function of the center-of-mass position h_G, the width satisfies the finite-size scaling form

$$w_{av}(h_G;L) \simeq L \psi \left(\frac{h_G}{L} \right) \tag{62}$$

where the scaling function $\psi(x)$ has for asymptotic behaviors $\psi(x \to \infty) = const$ and $\psi(x \to 0) \propto x$, so that in the transient regime, one has the simple proportionality

$$w_{av}(h_G;L) \underset{h_G \ll L}{\simeq} (const) \;\; h_G \tag{63}$$

The compatibility between the finite-size scaling forms of Eq. 58 and of Eq. 62 yields the following finite-size scaling form for the center-of-mass position

$$h_G(t;L) \simeq L H \left(\frac{t}{L^z} \right) \tag{64}$$

where $H(x)$ is a scaling function (data not shown).

G. Simple arguments to determine the exponents for $0 < \alpha < 1$

We expect that the roughness $\zeta = 1$ found above numerically for the special case $\alpha = 1/2$ remains the same in the whole phase $0 < \alpha < 1$ where strong non-self-averaging effects of the trapping times (Eq 45) occur

$$\zeta(0 < \alpha < 1) = 1 \tag{65}$$

We may now use a simple argument to determine the other exponents as a function of α in the interval $0 < \alpha < 1$. For h_G large, the time $t(h_G, L)$ needed to make a center-of-mass displacement of order h_G for a polymer of length L may be estimated from the maximal $\tau_{max}(N)$ trapping time among $N = (L h_G)$ independent variables drawn with the probability distribution of Eq 45

$$\tau_{max}(N) \sim N^{1/\alpha} \sim (L h_G)^{1/\alpha} \tag{66}$$

From this maximal trapping time, the minimal rate transition rate encountered is from Eq. 47

$$W_{out}^{min} \sim \frac{1}{\tau_{max}(L h_G)} \sim \frac{1}{(L h_G)^{1/\alpha}} \tag{67}$$

Assuming that the time t scales as the inverse of this minimal rate $t \sim 1/W_{out}^{min} \sim \times (L h_G)^{1/\alpha}$, we obtain by inversion the following scaling in the stationary regime

$$h_G(t;L) \underset{t \gg t^*(L)}{\simeq} \frac{t^{\alpha}}{L} \tag{68}$$

The scaling function $H(x)$ of Eq. 64 thus grows asymptotically as the power-law $H(x \to \infty) \sim x^\alpha$ and the dynamical exponent z describing the scaling of the crossover time $t^*(L) \sim L^z$ reads

$$z(\alpha) = \frac{2}{\alpha} \tag{69}$$

For $\alpha = 1/2$ used in our simulations, this corresponds to $z = 4$ in agreement with the value measured above (Eqs 60).

To determine the exponent β of the initial transient regime, the above argument has to be changed as follows. We expect that in the transient regime, an extensive number (ρL) of monomers (with a finite density ρ) are still pinned in their initial positions. Equivalently, there is a number ρL of segments of typical length $l_\rho \sim L/(\rho L) \sim 1/\rho$, that have made a move of typical amplitude $h_i \sim l$, because the dynamics is building the roughness $\zeta = 1$ at these small scales. As a consequence, the center-of-mass displacement is of order $h_G \sim \rho l_\rho^2 \sim l_\rho$. Since all these segments are independent, we now have to evaluate the time t_{l_ρ} for a single segment of size l_ρ to move over a distance of order l_ρ, i.e. the time t_{l_ρ} to overcome l_ρ^2 trapping times. The maximal trapping time among these scales as (see Eq. 66)

$$\tau_{max}(N_\rho = l_\rho^2) \sim N^{1/\alpha} \sim l_\rho^{2/\alpha} \tag{70}$$

The time t_{l_ρ} can be thus estimated as in Eq. 67 : $t_{l_\rho} \sim 1/W_{out}^{min} \sim \times l_\rho^{2/\alpha}$. Using $h_G \sim l_\rho$ derived above, we obtain by inversion the transient behavior

$$h_G(t; L) \underset{t \ll t^*(L)}{\simeq} t^{\frac{\alpha}{2}} \tag{71}$$

The scaling function $H(x)$ of Eq. 64 thus grows at the origin as the power-law $H(x \to 0) \sim x^{\alpha/2}$ i.e. the transient exponent β reads

$$\beta(\alpha) = \frac{\alpha}{2} \tag{72}$$

For $\alpha = 0.5$, this is in agreement with the value $\beta \sim 0.24$ measured above (see Eqs 56 and 61). Finally, with the values of Eqs 65, 69 and 72, the transient behavior of the width of Eq. 59 simplifies into the same scaling behavior as the center-of-mass displacement h_G (Eq. 71)

$$w_{av}(t; L) \underset{t \ll t^*(L)}{\simeq} t^{\frac{\alpha}{2}} \tag{73}$$

as expected from Eq. 63.

In conclusion, the dynamics in the zero-velocity phase $0 < \alpha < 1$ can be understood in terms of simple arguments based on the statistics of trapping times. The critical exponents that are computed from these arguments are in agreement with our numerical simulations both in the stationary regime and the transient regime.

V. COMPARISON WITH ROUGHNESS EXPONENTS MEASURED IN PREVIOUS WORKS

For a polymer with the metric constraint at finite temperature driven by a small force, we may summarize the behavior of the roughness discussed in the above sections as follows :

(i) at scales smaller than $l^*(T, F)$, the force is too small to really change the energy landscape seen by the polymer at $F = 0$, and thus the roughness is expected to be governed by the equilibrium value $\zeta_{eq} = 2/3$.

(ii) at scales larger than $l^*(T, F)$, we have found in our numerical study of the previous section that, at small force where the exponent of the trapping time power law (Eqs 29 and 30) is in the interval $0 < \alpha(F, T) < 1$, the roughness becomes $\zeta = 1$.

In this section, we compare this scenario with previous works.

A. Relation with other works finding a roughness exponent $\zeta = 1$ in the presence of a metric constraint

We are aware of two works where a roughness exponent $\zeta = 1$ has been measured for the dynamics in the presence of a metric constraint:

(i) Sneppen has found a roughness exponent $\zeta = 1$ for the following self-organized interface dynamics called 'model A' in [50] : at each iteration, the site with the smallest pinning force among the sites that are allowed to move without breaking the metric constraint, moves forward by one unit and a new pinning force is drawn for this site.

Self-organized-criticality models are usually not directly related to finite-temperature dynamics. Here for instance, the important differences with the effective directed traps model defined by the master equation of Eq. 11 with Eq. 47 are the following : in Sneppen's model, there is no real time, but only a number of iterations that corresponds to the total displacement h_G of the center-of-mass; and at each iteration, it is the always the least pinned movable site that moves, whereas in the master equation of Eq 11, the time and the site of the next moves are drawn with Eqs 50 and 51). Nevertheless, there is clearly a close relationship between the two models, in particular in the mechanism that generates a roughness exponent $\zeta = 1$ in the stationary state (see the typical configurations on Fig. 4 (a) of the present paper and Fig. 1a of Ref. [50]).

(ii) Tang and Leschhorn have found in their analysis of the dynamics slightly above the directed percolation depinning threshold [51, 52] that the moving interface is not self-affine, but is a mixture of two kinds of behaviors : there exists finite pinned segments that have for roughness the exponent of the depinning transition $\zeta_{dep} = \zeta_{DP} \sim 0.63$ whereas segments with a slope of order 1 are found between them.

Since the region discussed by Tang and Leschhorn is on the horizontal axis of Fig. 2 slightly above the depinning critical point, it is very far from the region near the vertical axis of Fig. 2 discussed in the present paper. However, the two pictures that emerge have nevertheless some similarities : in our case, the local roughness is determined by the equilibrium exponent $\zeta_{eq} = 2/3$ up to the length l^*, in their case the local roughness is the depinning roughness $\zeta_{dep} = \zeta_{DP} \sim 0.63$, but in both cases the roughness becomes equal to 1 at largest scales, i.e. the maximal roughness which is physically acceptable. This seems to indicate that in both cases, it is very difficult for the different regions of the polymer to remain synchronized during the dynamics, so that the maximal slope 1 allowed by the metric constraint is actually reached to maintain the full polymer together.

B. Roughness exponents measured in other works in the presence of an elastic energy

Most of the numerical studies on the dynamics at finite temperature have been done for a Langevin dynamics in the presence of an elastic quadratic energy between monomers :

(i) the equilibrium roughness exponent $\zeta_{eq} = 2/3$ has been measured during the driven dynamics in [14], and in [15] when the temperature remains larger that some disorder-dependent threshold. In our opinion, this means that in these two simulations, the length L of the polymer was smaller or of the order of the length $l^*(F,T)$.

(ii) at lower temperature in [15], the authors have measured an effective roughness exponent of order $\zeta \simeq 0.9$. In the study [16] concerning the limit $T \to 0$, the authors have found a crossover between the equilibrium value $\zeta_{eq} = 2/3$ at small scales and the critical depinning value $\zeta_{dep} \sim 1.26$ at larger scales, and have related this crossover to Functional RG calculations [53]. Since any roughness exponent $\zeta > 1$ is unphysical (see [54, 55] and the discussion in Appendix A), our opinion is that it would be very interesting if the simulations of [16] based on a quadratic elastic energy were done with the metric constraint instead, to see what physically acceptable roughness exponent $\zeta \leq 1$ would actually emerge at large scales.

VI. CONCLUSIONS AND PERSPECTIVES

In this paper, we have considered the dynamics of the directed polymer in a two-dimensional random potential in the regime where the temperature T is finite and the external force F is small. We have explained how the "infinite disorder fixed point" that describes the dynamics for $F = 0$ becomes a "strong disorder fixed point" for small F with an exponential distribution of renormalized barriers. Since the corresponding distribution of trapping times then only decays as a power-law $P(\tau) \sim 1/\tau^{1+\alpha}$, where the exponent $\alpha(F,T)$ vanishes as $\alpha(F,T) \propto F^{\mu}$ as $F \to 0$, we have concluded that the motion is only sub-linearly in time $h_G(t) \sim t^{\alpha(F,T)}$ in the region $\alpha(F,T) < 1$, i.e. that the asymptotic velocity vanishes $V = 0$, in contrast with the usual creep scenario where the velocity is finite as soon as $(T > 0, F > 0)$. All along the paper, we have discussed the similarities with the Sinai model with bias, where an analogous zero-velocity phase has been established long ago by rigorous methods [3, 4, 5, 6] and where the asymptotic exactness of the strong disorder renormalization has been demonstrated explicitly by a direct comparison with the available rigorous results [29, 32, 33]. We have then checked the presence of the predicted zero-velocity phase by numerical simulations of a directed polymer with a metric constraint driven in a traps landscape. We have moreover obtained that the roughness, which is governed by the equilibrium exponent $\zeta_{eq} = 2/3$ up to the large scale l^*, is equal to $\zeta = 1$ at the largest scales.

An important issue is of course whether such a zero-velocity phase also exists for interfaces of higher dimensionalities $d > 1$ driven in a random medium of dimension $(d+1)$, and more generally for other classes of driven extended systems. Since "collective transport in random media is an impossibly broad subject" [7], a general answer clearly goes beyond the present work. However we think that the essential property needed to have a zero-velocity phase at small force

is the presence of a positive barrier exponent $\psi > 0$ for the dynamics at $F = 0$, and this should be the case for a broad class of disordered systems in finite dimensions. Then the dynamics for $F = 0$ will be logarithmically slow and should correspond to some "infinite disorder fixed point" for the renormalized barriers, that transforms into a "strong disorder fixed point" at small F, with an exponentially distribution of renormalized barriers. Another argument in favor of this general scenario is the extremal statistics argument on the barriers [25, 28] that also lead to an exponential tail for the probability distribution of large barriers, and thus to a power-law decay for the trapping time distribution.

Acknowledgements

It is a pleasure to thank J.P. Bouchaud for sending us a copy of his conference proceeding [27].

APPENDIX A: TYPE OF INTERACTIONS : METRIC CONSTRAINT OR ELASTIC ENERGY

In the text, the interaction used to maintain the continuity of the interface is a metric constraint, both for the microscopic model and for the effective directed trap model described in section III D 3. In the present appendix, we explain this choice.

1. Subtleties in the choice of microscopic interactions

Let us first recall the two types of *microscopic interactions* that are usually considered in the literature for a polymer described by the heights $\{h_i\}$ of monomers :

a. Metric constraint between the heights of two neighboring monomers : $|h_{i+1} - h_i| \leq 1$.

This metric constraint is for instance very much used in numerical studies using transfer matrix methods (see the review [9]). It can can be moreover justified in various microscopic models, in particular when the directed polymer represents an interface in a two-dimensional disordered ferromagnet well below the critical temperature T_c, which was the original motivation to introduce the directed polymer model [10].

b. Elastic energy of the form : $E_{el}(h_{i+1} - h_i) \sim (h_{i+1} - h_i)^n$, *with* $n = 2$ *usually.*

It is of course very common in physics to replace a hard constraint by a soft constraint. In the present case, the use of an elastic quadratic energy usually comes from a small-gradient expansion, an hypothesis which has to be consistent with the results obtained for the roughness. Indeed, the roughness exponent ζ has to satisfy the bound $\zeta \leq 1$ for at least two reasons [54, 55] : first, if one obtains $\zeta > 1$, the gradient is not small, and thus there is an inconsistency with the small gradient expansion used to obtain the elastic quadratic energy ; second, if one obtains $\zeta > 1$, the elastic energy diverges in the thermodynamic limit $L \to \infty$.

c. Discussion

The metric constraint can be seen as the limit $n \to \infty$ of the power n of the elastic energy. As a consequence, there is room for various universality classes between $n = 2$ and $n = \infty$. So one should not assume a priori that all these interactions are equivalent, but test for each case of interest if they lead to the same results or not.

For the directed polymer at equilibrium at any temperature T and no external force in dimension $1 + 1$, the same equilibrium roughness exponent $\zeta_{eq} = 2/3$ arises if one considers the metric constraint or the elastic energy with $n = 2$ (see the review[9]). However, at the zero-temperature depinning transition (see Fig. 2), some subtleties arise (see the detailed discussion in [55]) : it turns out that the model defined in terms of an elastic quadratic energy (case $n = 2$) gives a roughness exponent $\zeta_{n=2} \sim 1.25$ which is unphysical because it is strictly greater than one $\zeta_{n=2} > 1$ [54, 55]. This is in contrast with the model defined either with the metric constraint or with an elastic energy of at least quartic order ($n \geq 4$) where the roughness exponent is physical $\zeta_{metric} \leq 1$ and actually takes a value $\zeta_{metric} \sim 0.63 \sim \zeta_{n=4}$ [55] that can be understood in terms of pinning by Directed Percolation clusters [51, 56].

In conclusion, since the microscopic model with an elastic quadratic energy (case $n = 2$) is known to lead to unphysical results at the depinning transition ($\zeta_{n=2} > 1$), it is clearly not a good starting point to study the general phase diagram for the dynamics at finite temperature and finite force. On the contrary, the metric constraint is always a safe choice, since by definition it cannot produce an unphysical roughness strictly larger than one.

2. Interaction between the segments of size $l^*(F,T)$ in the effective directed trap model

For the reasons explained in details above, we thus consider that the *microscopic* interactions between monomers are given by the metric constraint. The question is then : in the effective directed trap model described in section III D 3, what is the corresponding renormalized interactions between two consecutive segments of typical length $l^*(F,T)$ representing local quasi-equilibrated metastable states ? In the absence of more refined arguments, we feel that the metric constraint is actually also an appropriate renormalized interaction, since it prevents the appearance of an unphysical roughness $\zeta > 1$ and it allows all possible physically acceptable values $\zeta \leq 1$ for the roughness.

[1] P.W. Anderson, Phys. Rev. B 109, 1492 (1958).
[2] J.P. Bouchaud and A. Georges, Phys. Rep. 195, 127 (1990).
[3] H. Kesten, M. Koslov and F. Spitzer, Compositio Math 30, 145 (1975).
[4] B. Derrida and Y. Pomeau, Phys. Rev. Lett. 48, 627 (1982); B. Derrida, J. Stat. Phys. 31, 433 (1983); B. Derrida, Phys. Rep. 103, 29 (1984).
[5] M.V. Feigelman and V.M. Vinokur, J. Phys. France 49, 1731 (1988).
[6] J.P. Bouchaud, A. Comtet, A. Georges and P. Le Doussal, Ann. Phys. 201, 285 (1990).
[7] D.S. Fisher, Phys. Rep. 301, 113 (1998).
[8] T. Giamarchi, A. B. Kolton, A. Rosso, Lecture Notes in Physics 688, 91 (2006).
[9] T. Halpin-Healy and Y.C. Zhang, Phys. Rep. 254 (1995) 215.
[10] D. A. Huse and C. L. Henley, Phys. Rev. Lett. 54, 2708 (1985); D. A. Huse, C. L. Henley, and D. S. Fisher, Phys. Rev. Lett. 55, 2924 (1985).
[11] A.A. Middleton, Phys. Rev. E 59, 2571 (1999).
[12] J. Vannimenus and B. Derrida, J. Stat. Phys. 105,1 (2001).
[13] L.-W. Chen and M. C. Marchetti Physical Review B 51 6296 (1995) ; S. Bustingorry, A.B. Kolton and T. Giamarchi, EPL 81, 26005 (2008).
[14] H. G. Kaper, G. K. Leaf, D. M. Levine, and V. Vinokur Phys. Rev. Lett. 71, 3713 (1993).
[15] A.B. Kolton, A. Rosso, T. Giamarchi, Phys. Rev. Lett. 94, 047002 (2005).
[16] A.B. Kolton, A. Rosso, T. Giamarchi and W. Krauth, Phys. Rev. Lett. 97, 057001 (2006).
[17] C. Monthus and T. Garel, J. Phys. A: Math. Theor. 41, 115002 (2008).
[18] A. Kolton, A. Rosso and T. Giamarchi, Phys. Rev. Lett. 95, 180604 (2005).
[19] C. Monthus and T. Garel, arXiv:0802.2502.
[20] C. Monthus and T. Garel, arXiv:0804.1847.
[21] B. Derrida, Physica D 107, 186 (1997).
[22] J.P. Bouchaud and M. Mézard, J. Phys. A: Math. Gen. 30, 7997 (1997); G. Biroli, J.P. Bouchaud and M. Potters, J. Stat. Mech. (2007) P07019.
[23] A. Glatz, V. M. Vinokur, and Y. M. Galperin, Phys. Rev. Lett. 98, 196401 (2007).
[24] J.P. Bouchaud, J.Phys. I France 2, 1705 (1992); J.P. Bouchaud and D. Dean, J. Phys. I (France) **5** 265 (1995); A. Compte and J. P. Bouchaud, J. Phys. A: Math. Gen. 31 6113 (1998); B. Rinn, P. Maass, and J.P. Bouchaud, Phys. Rev. Lett. 84, 5403 (2000) and Phys. Rev. B 64, 104417 (2001); E.M. Bertin, J.-P. Bouchaud, Phys. Rev. E 67, 026128 (2003) and Phys. Rev. E 67, 065105(R) (2003).
[25] R. Rammal, J. Physique, 46, 1837 (1985).
[26] L.B. Ioffe and V.M. Vinokur, J. Phys. C 20, 6149 (1987).
[27] J. P. Bouchaud, "Pinning and correlations in the vortex phase" proceedings of Cargese summer school 1993: "Vortices in Superfluids" ed. N. Bontemps, (Kluwer 1994).
[28] V.M. Vinokur, M. C. Marchetti and L.W. Chen, Phys. Rev. Lett. 77, 1845 (1996).
[29] F. Igloi and C. Monthus, Phys. Rep. 412 (2005) 277.
[30] S.-K. Ma, C. Dasgupta, and C.-k. Hu, Phys. Rev. Lett. 43, 1434 (1979) ; C. Dasgupta and S.-K. Ma Phys. Rev. B 22, 1305 (1980).
[31] D. S. Fisher Phys. Rev. Lett. 69, 534-537 (1992) ; D. S. Fisher, Phys. Rev. B 50, 3799 (1994) ; D. S. Fisher, Phys. Rev. B 51, 6411-6461 (1995); D.S. Fisher and A. P. Young, Phys. Rev. B 58, 9131 (1998). D.S. Fisher, Physica A 263 (1999) 222.
[32] D. Fisher, P. Le Doussal and C. Monthus, Phys. Rev. Lett. 80 (1998) 3539 ; D. S. Fisher, P. Le Doussal and C. Monthus, Phys. Rev. E 59 (1999) 4795; C. Monthus and P. Le Doussal, Physica A 334 (2004) 78.
[33] C. Monthus, Phys. Rev. E 67 (2003) 046109.

[34] P. Le Doussal and C. Monthus, Phys. Rev. E 60 (1999) 1212.
[35] D. S. Fisher, P. Le Doussal and C. Monthus, Phys. Rev. E 64 (2001) 66107
[36] C. Monthus, Phys. Rev. E 68 (2003) 036114; C. Monthus, Phys. Rev. E 69, 026103 (2004).
[37] M.B. Hastings, Phys. Rev. Lett. 90, 148702 (2003).
[38] J. Hooyberghs, F. Igloi, and C. Vanderzande Phys. Rev. Lett. 90, 100601 (2003) ; J. Hooyberghs, F. Igloi, and C. Vanderzande, Phys. Rev. E 69 (2004) 066140.
[39] R. Juhasz, L. Santen and F. Igloi, Phys. Rev. E 72, 046129 (2005)
[40] R. Juhasz, L. Santen and F. Igloi, Phys. Rev. Lett. 94 (2005) 010601. R. Juhasz, L. Santen and F. Igloi, Phys. Rev. E 74, 061101 (2006).
[41] O. Motrunich, S.-C. Mau, D. A. Huse and D. S. Fisher, Phys. Rev. B 61, 1160 (2000).
[42] J.P. Bouchaud, cond-mat/9910387, published in 'Soft and Fragile Matter: Nonequilibrium Dynamics, Metastability and Flow', M. E. Cates and M. R. Evans, Eds., IOP Publishing (Bristol and Philadelphia) 2000, pp 285-304
[43] L. Berthier, V. Viasnoff, O. White, V. Orlyanchik, F. Krzakala in "Slow relaxations and nonequilibrium dynamics in condensed matter"; Eds: J.-L. Barrat, J. Dalibard, M. Feigelman, J. Kurchan (Springer, Berlin, 2003).
[44] A.J. Bray and M. A. Moore, in Heidelberg colloquium on glassy dynamics, J.L. van Hemmen and I. Morgenstern, Eds (Springer Verlag, Heidelberg, 1986).
[45] D.S. Fisher and D.A. Huse, Phys. Rev. B38, 386 (1988); D.S. Fisher and D.A. Huse, Phys. Rev B38, 373 (1988).
[46] D.S. Fisher and D.A. Huse, Phys. Rev. B43, 10728 (1991); T. Hwa and D. S. Fisher, Phys. Rev. B 49, 3136 (1994).
[47] A.B. Bortz, M.H. Kalos and J.L. Lebowitz, J. Comp. Phys. 17 (1975) 10.
[48] W. Krauth, " Introduction to Monte Carlo Algorithms" in 'Advances in Computer Simulation' J. Kertesz and I. Kondor, eds, Lecture Notes in Physics (Springer Verlag, 1998); W. Krauth, " Statistical mechanics : algorithms and computations", Oxford University Press (2006).
[49] A.L. Barabási and H.E. Stanley, "Fractal concepts in surface groth", Cambridge University Press (1995).
[50] K. Sneppen, Phys. Rev. Lett., 69, 3539 (1992)
[51] L.H. Tang and H. Leschhorn, Phys. Rev. A 45, R8309 (1992).
[52] H. Leschhorn, Phys. Rev. E 54, 1313 (1996).
[53] P. Chauve, T. Giamarchi, and P. Le Doussal, Phys. Rev. B 62, 6241 (2000)
[54] H. Leschhorn and L.H. Tang, Phys. Rev. Lett. 70, 2973 (1993).
[55] A. Rosso and W. Krauth, Phys. Rev. Lett. 87, 187002 (2001); A. Rosso, A. K. Hartmann and W. Krauth, Phys. Rev. E 67, 021602 (2003).
[56] S.V. Buldyrev and al. Phys. Rev. A 45, R8313 (1992); S.V. Buldyrev, S. Havlin and H.E. Stanley, Physica A 200, 200 (1993).